Original Paper

Bubble removal from glass melts: Power-law model

Pavel Hrma

Department of Materials Science and Engineering, Case Western Reserve University, Cleveland, OH (USA)

An attempt is presented to understand published experimental results regarding bubble removal from molten glass, such as an exponential decrease in bubble count with time at constant temperature, in terms of the behavior of individual bubbles and bubble size distribution. It is assumed that bubbles of all sizes within a given range are initially randomly distributed in space; no new bubbles form at $t > 0$; the bubble growth/shrinkage rate depends on bubble radius according to a simple power-law relation; and each bubble rises to the melt surface with a velocity proportional to the square of its radius. The time dependence of bubble size distribution, including the maximum and minimum sizes and the total removal time, is determined. In particular, it is shown that an exponential decrease in bubble count requires either an improbable initial bubble size distribution or an unusual bubble growth/shrinkage history. Moreover, the exponential (or similar to exponential) decrease in bubble count is incompatible with both the constant bubble growth rate as observed experimentally for a multibubble mixture and bubble growth rate proportional to the reciprocal bubble radius as predicted theoretically for an isolated bubble. It is suggested that the bubble number observed in refining experiments is, in the final stage, controlled by bubble generation on the container walls.

Entfernung von Blasen aus der Glasschmelze – Potenzgesetzmodell

Es wird ein Ansatz vorgestellt, um Ergebnisse aus der Literatur zur Beseitigung von Blasen aus Glasschmelzen hinsichtlich des Verhaltens einzelner Blasen und der Blasengrößenverteilung zu verstehen, wie z. B. eine zeitabhängige exponentielle Abnahme der Blasenanzahl bei konstanter Temperatur. Es wird angenommen, daß Blasen unterschiedlicher Größe innerhalb eines vorgegebenen Bereiches einer zufälligen räumlichen Verteilung unterliegen, daß sich bei $t > 0$ keine neuen Blasen bilden, daß die Wachstums- bzw. Schrumpfungsgeschwindigkeit der Blasen nach einer Potenzfunktion vom Blasenradius abhängt und daß jede Blase mit einer zum Quadrat ihres Radius proportionalen Geschwindigkeit an die Schmelzoberfläche aufsteigt. Die Zeitabhängigkeit der Blasengrößenverteilung, einschließlich der minimalen und maximalen Größen sowie der Gesamtzeit bis zur Beseitigung der Blasen, wird bestimmt. Insbesondere wird gezeigt, daß eine exponentielle Abnahme der Blasenanzahl entweder eine unrealistische Anfangsverteilung der Blasengrößen oder eine ungewöhnliche Vorgeschichte des Blasenwachstums bzw. des Blasenschrumpfens voraussetzt. Außerdem ist die exponentielle (oder die einer exponentiellen ähnliche) Abnahme der Blasenanzahl weder vereinbar mit der konstanten Wachstumsgeschwindigkeit, wie sie experimentell bei einem Blasenensemble beobachtet wird, noch mit dem für Einzelblasen theoretisch vorausgesagten Befund, daß die Wachstumsgeschwindigkeit umgekehrt proportional zum Blasenradius ist. Es wird angenommen, daß die bei Läuterexperimenten beobachtete Blasenanzahl im Endstadium durch die Entstehung von Blasen an den Behälterwänden bestimmt wird.

1. Introduction

The kinetics of bubble removal from molten glass appears to be the most prominent aspect of the refining process [1]. It involves bubble nucleation, growth or shrinkage, motion through the melt, and coalescence. Nucleation takes place on solid-liquid interfaces provided by undissolved refractory batch particles and container walls. Growth or shrinkage are caused by diffusion of gases in or out of the bubble, from or to the surrounding melt. Bubble motion is driven by buoyancy and is affected by flow of melt and the presence of other bubbles. The complexity of the process makes it difficult to develop a general model for bubble removal from glass melts. The commonly adopted simplifications are:

a) no new bubbles are produced after all batch solids dissolve,

b) mutual interaction of bubbles does not occur,

c) bubbles move vertically upward, and

d) change their size according to a simple formula.

Since bubbles seem to be quite prone to nucleate on the container walls, the assumption most likely not to be satisfied in laboratory melts is that of no bubble formation after the batch-free time. Formation of bubbles from gas-oversaturated melts on ceramic refractory walls is well documented [2]. Němec and Žlutický [3] photographically recorded a massive production of bubbles when a ceramic refractory material was introduced to a gas-oversaturated melt. Cable [4] observed that melts in ceramic crucibles contain more bubbles than melts in platinum crucibles. Obviously, this can be caused by differences in bubble production rate from different wall materials. Němec [5], who used silica glass crucibles, found it necessary to prevent bubble nucleation on the bottom by placing in the crucible a 5 mm layer of prerefined glass before charging the batch.

Received 17 October 1988, revised manuscript 19 April 1989.

Nevertheless, formation of new bubbles after the batch-free time has been disregarded by investigators. Cable [6], who studied refining of glass for many years, came to the conclusion that bubble formation on the bottom and the walls of the crucible during refining experiments is unimportant. Likewise, van Erk, Papanikolau, and van Pelt [7] based their analysis on the assumption of no bubble formation after the batch-free time. The argument given for disregarding the bubbles generated on crucible walls in refining studies is that the number of these bubbles makes only a tiny fraction of the number of bubbles nucleated on batch particles. Even after all batch particles are completely dissolved, the fraction of bubbles produced at container walls remains relatively small.

However, an objection can be raised against this reasoning. Towards the end of the bubble removal process, the ratio between bubbles from batch particles and those from walls may change and even reverse. Eventually, after a long refining time, a considerable portion of bubbles in the melt may consist of those coming from crucible walls. If this is so, the applicability of laboratory bubble counts to refining in industrial furnaces will become problematic. In large industrial furnaces, most of the melt is far away from refractory walls, and thus only bubbles nucleated on batch particles are present and have to be removed. If bubbles were generated on the container walls in crucible experiments after all batch nucleated bubbles have been removed, it will lead to an error in the determination of the refining time.

The question about the significance of bubble generation after the batch-free time can be answered either experimentally, by looking for evidence of bubble nucleation or its absence on the container walls, or mathematically, by showing whether or not the data from bubble removal measurements are compatible with the assumption of no bubble generation. The latter method was adopted in this paper.

The remaining three assumptions, that is, no mutual interaction of bubbles, buoyancy-driven bubble motion, and time-dependent bubble size, do not impose such severe restrictions as does the generation of new bubbles. Mutual interaction of bubbles will occur if the refining process is vigorous, that is, if bubble number density per unit volume is large and if bubbles grow rapidly. A very vigorous refining can even generate foam. Němec [3 and 5] has shown that if the bubble density is large, the bubble-melt mixture is in a turbulent motion and coalescence is frequent. While large bubbles move upward, some smaller bubbles move downward due to countercurrent flows of glass. However, at small bubble densities, as Cable [6] pointed out, bubbles move relatively independently and coalescence is negligible. Therefore, disregarding bubble interaction will affect the initial stages of refining, but not the removal of the last bubbles, which is crucial for the overall bubble removal time. Likewise, the Stokesian behavior of bubbles will be applicable at the final stages of refining when bubbles no longer affect each other.

The reason why the question of bubble generation after the batch-free time is difficult to answer lies in the fact that bubbles change their size. A bubble leaving the melt a long time after the disappearance of the last solid particles could either have been nucleated on a container wall or could have survived as a small, slowly moving bubble which has grown larger. Therefore, a wide range of possibilities of bubble behavior regarding their growth or shrinkage is considered in this paper.

Bubble growth is determined by the bubble history after nucleation. This history can be rather complex because of the presence of multiple gases and the dependence of the activities of these gases and the temperature on position and time. According to Němec [8], the bubble growth rate at refining temperatures was approximately constant in all cases of homogeneous and isothermal melts investigated. Furthermore, at lower temperatures, bubbles tend to dissolve. A more complex behavior was suggested by other investigators. Cable [6] reasoned that small bubbles may dissolve while large bubbles grow, whereas van Erk et al. [7] inferred that all bubbles grow, but large bubbles grow faster than smaller ones.

Nonlinear bubble growth can be expected with multiple gases, or if capillary forces compete with pressure forces, or if the temperature of melt changes with time. If gas B diffuses into a bubble filled with an extremely slowly diffusing gas A, the partial pressure of gas B in the bubble will increase with increasing bubble size and this would diminish the driving force for further growth. If gas B diffuses out of the bubble containing a small amount of gas A, the bubble volume will initially decrease rapidly and then slowly. Bubbles that are so small that the partial pressure of the refining gas is comparable to the capillary pressure within the bubble will either grow or shrink, according to which pressure is dominating, initially slowly, but at an increasing rate as the radius differs more and more from its critical value.

The time dependence of radius for both stationary and moving bubbles was calculated by many authors, most recently by Weinberg et al. [9 to 12], Cable and Frade [13 and 14], and Beerkens [15]. The variation in behavior is large and the mathematics involved is complex. Solving a set of differential equations for concentration and velocity fields around a bubble, subjected to complex boundary conditions, is the most exact method, but it is laborious and time-consuming. A simplified method developed by Beerkens [15], based on correlations for mass transfer coefficient, is less rigorous, but sufficiently accurate and more flexible, allowing incorporation of the effects of

chemical reactions and changing temperature. An even simpler approach was adopted by Němec and Mühlbauer [16 and 17], who regarded the mass transfer coefficient as a temperature-dependent constant.

In the present work the bubble radius versus time variation is approximated by a simple power-law function. Despite its simplicity, a power-law function is able to cover a wide range of bubble behavior, including constant size, growth, or shrinkage. The rate of growth or shrinkage can be constant or dependent on bubble radius. The power-law function enables one to express analytically the time change of maximum and minimum bubble sizes present in the melt during refining, the bubble removal time, and the bubble number distribution. Thus, the experimentally determined bubble count can be matched with the behavior of individual bubbles, provided that the assumptions of no bubble nucleation and independent bubble motion are valid.

The following ideal situation of bubble removal will be considered.

1) A layer of liquid contains initially ($t = 0$) bubbles that are randomly but uniformly distributed in space and arbitrarily distributed in size. Hence, the spatial bubble number density for each size is independent of position within the liquid layer.

2) The layer is confined within the top surface of the liquid and a horizontal plane which may or may not be the container bottom. If this plane is not the bottom, the liquid below it is bubble-free.

3) At $t > 0$, the bubbles are subjected to gravity and rise up independently of each other without coalescence.

4) No new bubbles are formed at $t > 0$.

5) During their rise, bubbles change their size according to a power-law function relating the growth rate of a bubble to its actual size.

6) Bubbles disappear when they reach the top surface. The decrease in the top surface level due to bubble removal is disregarded.

The goal of this paper is to determine the bubble size distribution, especially the maximum and minimum size of the bubble population and the total bubble count as a function of time. The total bubble removal time as a function of the initial radius is also determined. These characteristics are affected by the parameters of the power-law function describing the bubble growth rate. On the other hand, bubble growth rate can be measured or predicted numerically. Therefore, the present analysis provides a step towards understanding the relationship between behavior of individual bubbles and removal of a bubble population from a volume of liquid. Eventually, it is shown that the assumption of no new formation of bubbles at $t > 0$ is usually invalid if applied to bubble count data from crucible melts.

2. Analysis

Consider an infinite horizontal layer of a bubble-liquid mixture of thickness h with a free top surface. At $t = 0$, the bubble size distribution is independent of position within the layer and at $t \geq 0$, no new bubbles are generated. Bubbles move due to buoyancy vertically upwards, with velocity proportional to the square of their radii,

$$v = k_s r^2, \tag{1}$$

where $k_s = k_1 g \varrho/\mu$. *Here* g is the gravitational acceleration, ϱ the bubble-free liquid density, μ the viscosity, and k_1 a coefficient given by Stokes' or Hadamard's formula. Note that k_s is the same for all bubbles, which implies that bubbles do not affect each other and do not coalesce.

Next, bubbles grow or shrink with the rate dependent on their radius, that is,

$$dr/dt = f(r)\,, \tag{2}$$

where the function f is the same for all bubbles regardless of their original position and size. This assumption eliminates the role of the history as the determining factor for the growth rate, but functions f can be chosen so as to represent typical or interesting situations.

Equations (1 and 2) imply that at $t > 0$ all bubbles of the same initial size ascend always with the same velocity and, since their growth rates are identical, they are equal in size. The position of a bubble which at $t = 0$ was at a distance h from the top surface depends on time by $x_r = h - {}_0\int^t v\,\mathrm{d}t$, or, using equation (1),

$$x_r = h - k_s \int_0^t r^2\,\mathrm{d}t\,. \tag{3}$$

For $\mathrm{d}r/\mathrm{d}t \neq 0$, this can be rearranged using equation (2):

$$x_r = h - k_s \int_{r_0}^{r} r^2\,(\mathrm{d}r/\mathrm{d}t)^{-1}\,\mathrm{d}r\,, \tag{4}$$

where $r_0 = r(0)$ is the initial radius.

If there are no bubbles below the depth h at $t = 0$, the time for bubbles of initial radius r_0 to disappear entirely from the liquid, t_h, and the corresponding final radius, r_h, follow from equations (3 and 4) by substituting $x_r = 0$:

$$h / k_s = \int_0^{t_h} r^2\,\mathrm{d}t \tag{5}$$

and

$$h / k_s = \int_{r_0}^{r_h} r^2\,(\mathrm{d}r/\mathrm{d}t)^{-1}\,\mathrm{d}r\,. \tag{6}$$

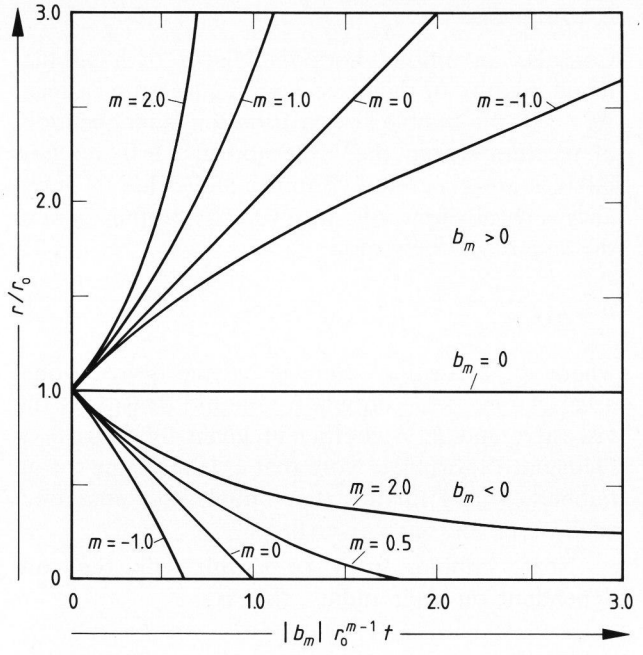

Figure 1. Normalized bubble radius r/r_0 as a function of normalized time $|b_m| r_0^{m-1} t$ represents bubble growth or shrinkage for different values of m and b_m.

It is convenient for further analysis to adopt for the bubble growth rate the power-law function

$$dr/dt = b_m r^m, \tag{7}$$

where b_m and m are constants. By choosing different values for b_m and m, a large variety of bubble behavior can be covered. However, the power-law function (7) does not produce maxima or minima of bubble sizes. Such phenomena can be introduced by a polynomial function, but this possibility will not be pursued in this paper.

Integration of equation (7) yields:

$$r = [r_0^{-m+1} - (m-1)\, b_m\, t]^{-1/(m-1)} \text{ for } m \neq 1\,, \tag{8}$$

$$r = r_0 \exp(b_1\, t) \text{ for } m = 1\,. \tag{9}$$

An inspection of equation (8) shows (figure 1) that if $b_m > 0$, bubbles grow, while the growth rate increases with time for $m > 0$, decreases for $m < 0$, and is constant for $m = 0$. Further, if $b_m < 0$, bubbles shrink, while the shrinkage rate increases with time for $m < 0$, decreases for $m > 0$, and is constant for $m = 0$. Finally, if $b_m = 0$, bubble size remains unchanged.

It also follows from equations (8 and 9) that at the time

$$t_{\max} = (m-1)^{-1}\, b_m^{-1}\, r_0^{-m+1} \tag{10}$$

$r \to \infty$ for growing bubbles with $m > 1$ or $r \to 0$ for shrinking bubbles with $m < 1$. Therefore, $t_{\max}$ is the maximum lifetime for growing bubbles with $m > 1$, and the actual lifetime for shrinking bubbles with $m < 1$. Physically, shrinking bubbles with $m < 1$ collapse, whereas growing bubbles with $m > 1$ convert the bubbly liquid into foam as $t \to t_{\max}$. Otherwise, bubbles reach the top surface at the time

$$t_h = (m-1)^{-1}\, b_m^{-1}\, [r_0^{-m+1} - r_h^{-m+1}] \text{ for } m \neq 1, \tag{11}$$

$$t_h = b_1^{-1} \ln (r_h / r_0) \text{ for } m = 1\,, \tag{12}$$

where

$$r_h = [r_0^{-m+3} - (m-3)\, b_m h / k_s]^{-1/(m-3)} \text{ for } m \neq 3, \tag{13}$$

$$r_h = r_0 \exp(b_3\, h / k_s) \text{ for } m = 3\,. \tag{14}$$

Equations (11 to 14) follow from introducing equations (7 to 9) into equations (5 and 6). Equations (11 and 12) determine the time at which the last bubbles (that is, those initially located in the depth h) of the initial radius r_0 leave the liquid. Equations (13 and 14) predict the radius of these bubbles at the moment they reach the top surface of the liquid. The real lifetime of bubbles in the liquid is limited either by $t_{\max}$ or by t_h, whichever is shorter.

Figures 2a to l show twelve examples of bubble histories during their lifetime represented as normalized $\tilde{r}(\tilde{t})$ functions determined by three parameters: b_m, m, and r_0. Normalized variables,

$$\tilde{r} = r(|b_m|\, h / k_s)^{1/(m-3)}$$

and

$$\tilde{t} = t\, |b_m|^{2/(-m+3)}\, (k_s / h)^{(m-1)/(m-3)}$$

are used ($|b_m|$ denotes the absolute value of b_m). The lines representing the change of the bubble radii with time start from the initial bubble radius, $r = r_0$, at $t = 0$. Some of them end at the line $r_h(t)$, which represents the radius at which the last bubbles (initially placed at the depth h) of a given initial size leave the melt. The intersection of the line $r(t)$ with $r_h(t)$ determines also the time, t_h, of total removal of bubbles of a given initial radius through the top surface. At extreme situations, some bubbles grow to infinity before they reach the top surface (figure 2f) or leave the liquid only after an extremely long time (figures 2c to f and i to l). Shrinking bubbles which do not leave the melt through the top surface collapse when $r = 0$ (figures 2g and h).

Examples of growing bubbles ($b_m > 0$) with $m < 1$ are shown in figures 2a and b. It is assumed that the radii of all bubbles are confined within the range limited by $r_{\min}$ and $r_{\max}$. As bubbles grow and leave the melt, this range changes with time. Removal of bubbles proceeds in two stages. In the first stage, lasting for the time interval $t \in (0, t_1)$ (figure 2a), both minimum and maximum bubble

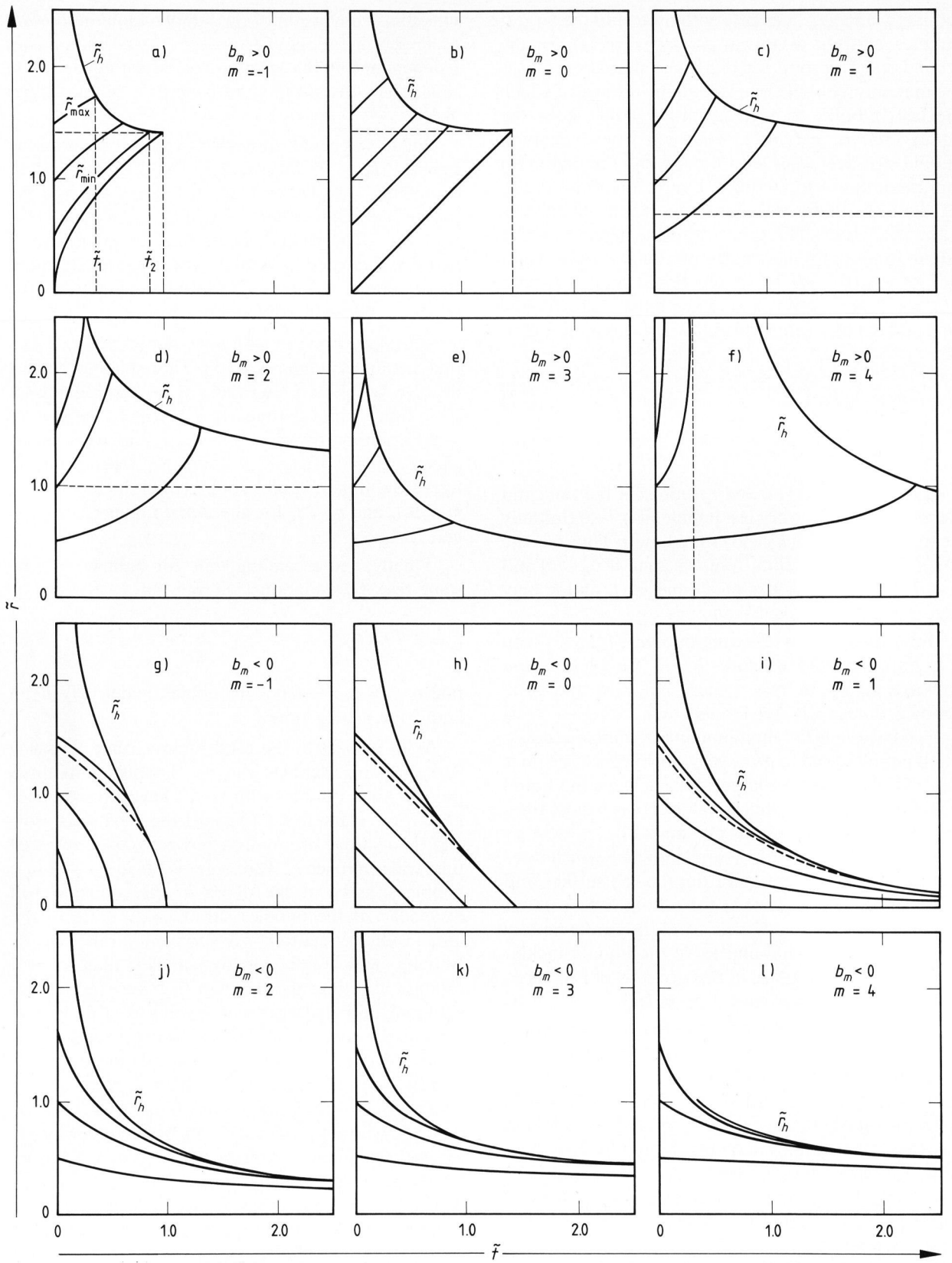

Figures 2a to l. Lifetime of bubbles in the melt represented as normalized $\tilde{r}(\tilde{t})$ functions for different initial sizes and growth or shrinkage parameters. a) and b) Bubble growing with $m = -1$ and $m = 0$, respectively; c) to f) bubble growing with $m \geq 1$; g) and h) shrinkage of bubbles which either dissolve completely or leave the liquid through the top surface; i) to l) shrinkage of bubbles which cannot dissolve completely ($m \geq 1$).

radii, r_{min} and r_{max}, increase with time until the largest bubbles entirely disappear at t_1 (figure 2a). In the second stage, lasting for the time interval $t \in (t_1,t_2)$, the maximum bubble size is given by the size at which the last bubbles of a given initial radius leave the liquid, that is, $r_{max} = r_h$. Therefore, the maximum bubble size decreases with time, while the minimum radius continues to increase. Eventually, both radii, r_{min} and r_{max}, become equal at t_2 when all bubbles leave the liquid. The times t_1 and t_2 depend on the original minimum and maximum bubble radii. Bubbles of $r_{min}(0) \to 0$ leave the liquid at $t_2 = t_c$ with $r_{min} = r_{max} = r_c$, where t_c and r_c are the characteristic time and the characteristic radius. By equations (11 to 14),

$$t_c = |(m-1)\, b_m|^{-1} r_c^{-m+1}, \tag{15}$$

$$r_c = [|(m-3)\, b_m|\, h / k_s]^{-1/(m-3)}. \tag{16}$$

If $b_m > 0$ and $m < 1$, t_c and r_c represent the time and radius at which the very last bubble of $r_0 \to 0$ (initially located at the depth h) leaves the liquid. Thus t_c is the upper limit for the total removal time if $b_m > 0$ and $m < 1$. For other values of b_m and m, t_c and r_c may have different physical meanings.

Four examples of growing bubbles ($b_m > 0$) with $m \geq 1$ are depicted in figures 2c to f. Bubble removal proceeds again in two stages, but now the total removal time, t_t, is not limited by t_c, for $t_t \to \infty$ as $r_{0min} \to 0$ (r_{0min} is the minimum initial bubble radius). Small bubbles tend to grow very slowly and large ones very rapidly, and thus large bubbles leave the liquid within a short time, while small bubbles persist for a long time. By equations (13 and 14), $r_h \to \infty$ as $h \to \infty$, which implies that small bubbles, which were initially located far enough from the top surface and have survived in the liquid for a long time without substantially changing position and size, grow rapidly at the end of their life and leave the liquid quickly. The behavior of bubbles in this group is of two types according to whether $m < 3$ or $m \geq 3$.

If $1 \leq m < 3$, bubbles tend to reach a fixed range of bubble sizes with progressing time (figures 2c and d). Accordingly, the final radius at which the bubbles of zero original size leave the melt approaches a constant value, that is, $r_h \to r_c$ as $t \to \infty$ (see the horizontal dotted lines in figures 2c and d). If $m \geq 3$, the bubble size range shrinks to zero as $t \to \infty$, that is, $r_h \to 0$ (figures 2e and f). Interestingly, as follows from equations (5 and 8), bubbles initially located at $h \geq h_c$, where

$$h_c = (m-3)^{-1} b_m^{-1} k_s r_0^{-m+3}, \tag{17}$$

can never reach the top surface because as $h \to h_c$, these bubbles grow to infinity. For a given depth, h, bubbles initially larger than r_c, will grow without limit by the time t_c (the dotted line in figure 2f). This can be viewed as conversion of the bubbly liquid into foam, as already mentioned. However, the assumptions of independent bubble motion, on which equation (1) rests, and constant mixture height, h, will no longer apply.

Figures 2g and h show two examples of shrinking bubbles ($b_m < 0$) with $m < 1$. These bubbles either completely dissolve or leave the liquid through the top surface. Thus either $t_t = t_m$ if $r_{0max} \leq r_c$ or $t_t = t_h$ if $r_{0max} > r_c$. The radius versus time for a bubble of $r_0 = r_c$ is indicated by dotted lines in figures 2g and h. By equations (13 and 17), bubbles initially located below $x_r = h_c$ will completely dissolve.

Shrinking bubbles with $m \geq 1$ are represented by four examples in figures 2i to l. These bubbles cannot dissolve completely and there is no upper limit for their total removal time. If $3 > m \geq 1$, bubbles of $r_0 \leq r_c$ neither dissolve nor reach the top surface (figures 2i and j); $t_h \to \infty$ as $r_0 \to r_c$ (dotted line in figure 2i). If $m \geq 3$, all bubbles reach the top surface at $t_h \leq t_c$ and $r_h < r_c$ for any initial radius (figures 2k and l).

Finally, the ascending time for bubbles of constant size, by equation (5), is

$$t_h = r^{-2} h / k_s ; \tag{18}$$

thus $t_h \to \infty$ as $r \to 0$ (small bubbles tend to stay in the liquid for a long time).

With respect to the total removal time, growing and shrinking bubbles can be classified into three groups. First, bubbles with $m < 1$ have a finite upper limit for t_t, namely $t_t \in (0,t_c)$. If these bubbles grow and their initial size approaches zero, their removal time will approach t_c. The larger is the initial size of a bubble situated at the depth h, the sooner it will disappear. If the bubbles shrink, only those of the initial radius equal to r_c will survive until the time t_c. Bubbles with radii initially smaller than r_c will collapse at a time shorter than t_c. Likewise, bubbles with radii initially larger than r_c will leave through the top surface at a time shorter than t_c. Second, for bubbles with $m > 3$, the total removal time cannot be shorter than t_c, but it is not limited from above: $t_t \in (t_c,\infty)$. Only bubbles initially larger than r_c can be removed without producing foam before reaching the top surface. Finally, bubbles with $1 \leq m \leq 3$ can be totally removed at any time, that is, $t_t \in (0,\infty)$, dependent on their initial radius. Combining these groups with the possibility that bubbles grow or shrink, and considering the case of constant size bubbles, the power-law model describes seven classes of bubble removal behavior that cover many simple real or conceivable situations.

Finite total removal time is associated with bubbles that

a) grow or shrink with $m < 1$, or

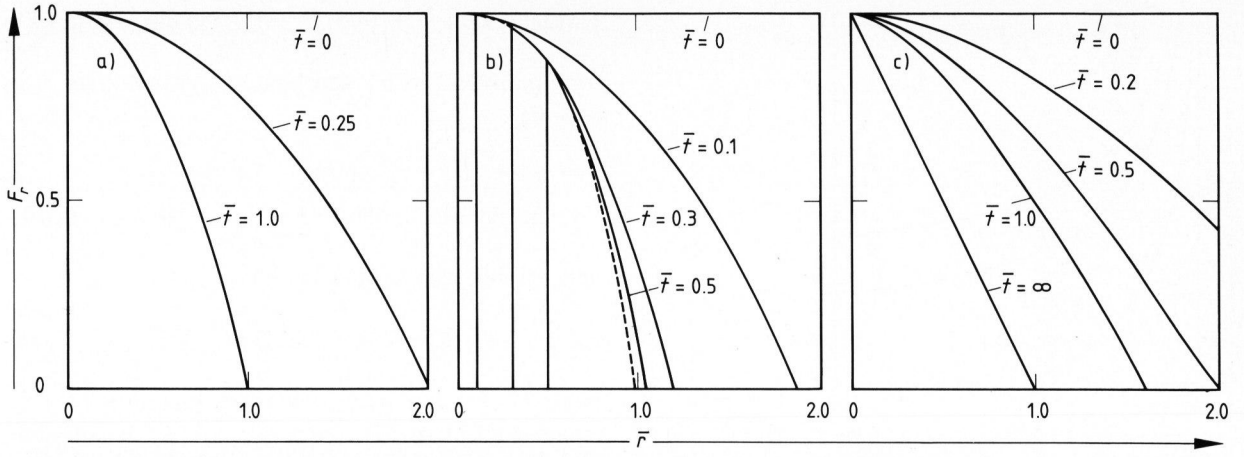

Figures 3a to c. Bubble size distribution function. Normalized count of bubbles with initial radius as a function of the bubble radius $\bar{r} = r / r_c$ with $\bar{t} = t / t_c$ and m as parameters; a) constant bubble size ($m \to \infty$), b) constant bubble growth rate ($m = 0$), c) accelerated bubble growth rate ($m = 2$).

b) do not shrink and have non-zero initial size, or c) shrink and either $1 \leq m < 3$ and $r_{0\min} > r_c$, or $m \geq 3$ and $r_{0\min} > 0$.

If these conditions are not satisfied, bubbles are not totally removed. The maximum initial size of bubbles that cannot be removed approaches zero at long times for bubbles that, first, grow with $1 \leq m < 3$ and $r_{0\min} \to 0$, or second, shrink either with $1 \leq m < 3$ and $r_{0\min} \leq r_c$, or with $m \geq 3$ and $r_{0\min} \to 0$. The maximum size approaching $r_c > 0$ at long times is associated with bubbles that grow with $1 \leq m < 3$ and $r_{0\min} \to 0$. Only these hypothetical bubbles are truly unremovable, but they cannot occur in reality because very small bubbles tend to collapse due to capillary forces.

A question arises as to how the number of bubbles of a given initial or instantaneous radius (there is a one-to-one correspondence between them defined by equations (8 and 9)) changes with time. Let N be the total number of bubbles per unit top surface area and $N_r = \partial N / \partial r$ the bubble size density (r is the instantaneous bubble radius). Since there are no bubbles below the depth h at $t = 0$,

$$N_r(t) = N_{r0}\, F_r(t)\,, \tag{19}$$

where $N_{r0} = N_r(0)$ is the initial bubble size distribution and $F_r = x_r / h$. For a uniform initial bubble size distribution (that is, if N_{r0} is independent of r), F_r is proportional to the actual bubble size distribution. By equation (3),

$$F_r = 1 - (k_s / h) \int_0^t r^2 \, \mathrm{d}t\,. \tag{20}$$

Substituting from equations (8 and 9) and integrating,

$$F_r = 1 - (k_s / h)\, b_m^{-1}\, (m-3)^{-1} \cdot \\ \cdot \left[r_0^{-m+3} - (r_0^{-m+1} - (m-1)\, b_m\, t)^{(m-3)/(m-1)}\right]. \tag{21}$$

By equation (19), F_r represents the normalized count of bubbles ($F_r(t) = N_r(t) / N_{r0}$) of a particular initial radius. Using equation (8), F_r can be expressed in terms of the instantaneous bubble radius at the time t as

$$F_r = 1 + (k_s / h)\, b_m^{-1}\, (m-3)^{-1} \cdot \\ \cdot \left[r^{-m+3} - (r^{-m+1} + (m-1)\, b_m\, t)^{(m-3)/(m-1)}\right]. \tag{22}$$

In particular, for bubbles of constant size ($b_m = 0$)

$$F_r = 1 - (k_s / h)\, r^2\, t\,, \tag{23}$$

for bubbles of constant growth rate ($m = 0$, $b_0 > 0$)

$$F_r = 1 - (k_s / h)\, (r^2\, t - b_0\, r\, t^2 + b_0^2\, t^3 / 3)\,, \tag{24}$$

for bubbles with accelerated growth ($m = 2$, $b_2 > 0$)

$$F_r = 1 - (k_s / h)\, r\, [b_2 + (r\, t)^{-1}]^{-1}, \tag{25}$$

and for bubbles growth rate proportional to r^{-1}

$$F_r = 1 - (k_s / h)\, (r^2\, t - b_{-1}\, t^2)\,. \tag{26}$$

Relation (23) was previously obtained by Cable [6] and equation (24) by Němec [18].

Figures 3a to c show how F_r depends on bubble radius and time for constant-size bubbles (figure 3a) ($m \to \infty$, which for 'growing' bubbles is equivalent to $b_m = 0$, see the trend in figure 1), constant growth-rate bubbles (figure 3b) ($m = 0$, $b_0 > 0$), and accelerated growth-rate bubbles (figure 3c) ($m = 2$, $b_2 > 0$). As the largest bubbles disappear from the liquid, the bubble size range recedes from the right for each of these examples. If the bubble size is constant (figure 3a), the left side of the bubble size

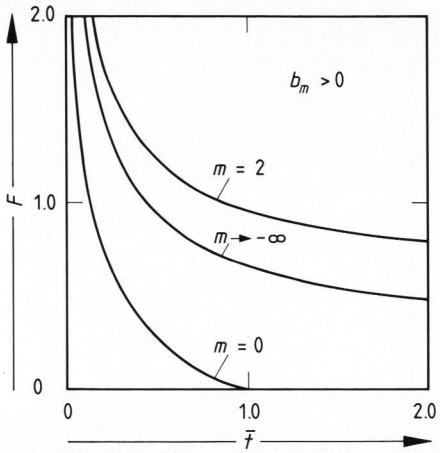

Figure 4. Bubble number decrease function; $\bar{t} = t / t_c$.

range is given by the smallest bubbles present in the liquid. If the bubble growth rate is constant, no bubble can be smaller than $r = b_0 t$ (the dotted line in figure 3b). Then $F_r = 0$ everywhere on the left side of the intersection of the dotted line with the $F_r(r,t)$ curve. All bubbles must disappear from the liquid by the time $t = (3 h / b_0^2 k_s)^{1/3}$ (compare figures 2b and 3b). In the case of accelerated growth (figure 3c), a constant size distribution is obtained at long times. This result agrees with figure 2d, according to which bubbles of a nonzero size can exist in the liquid after an arbitrarily long time.

The total number of bubbles is given by the integral

$$N = \int_{r_{\min}}^{r_h} N_r \, dr = \int_{r_{\min}}^{r_h} N_{r0} \, F_r \, dr \, . \tag{27}$$

The limits are, of course, the minimum and maximum radius of the bubbles present in the liquid at the time t, r_h being the radius of bubbles for which $t = t_h$ (all bubbles for which $t_h > t$ have been removed).

The integral in equation (27) can be evaluated analytically for a uniform initial bubble size distribution ($N_{r0} = \text{const.}$). Denoting

$$F = r_c^{-1} \int_{r_{\min}}^{r_h} F_r \, dr,$$

equation (27) can be rewritten as

$$N = r_c \, N_{r0} \, F \, , \tag{28}$$

where r_c is given by equation (16). Taking $r_{0\min} = 0$ and using equations (8, 9, 13, 14 and 23 to 26) one obtains for bubbles of constant size ($b_m = 0$)

$$F = (2/3) \, \bar{t}^{1/2} \, ; \tag{29}$$

for bubbles of constant growth rate ($m = 0$, $b_0 > 0$)

$$F = (1/12) \, \bar{t} \, [(4 - \bar{t}^3) \, ((4/3) \, \bar{t}^{-3} - 1/3)^{1/2} + 3 \, (\bar{t}^3 - 2)] ; \tag{30}$$

for bubbles with accelerated growth ($m = 2$, $b_2 > 0$)

$$F = 1/4 + (1/2 + \bar{t}^{-1}) \, (1/4 + \bar{t}^{-1})^{1/2} - \bar{t}^{-2} \cdot \\ \cdot \ln \{1 + (1/2) \, \bar{t} \, [1 + (1 + 4 \, \bar{t}^{-1})^{1/2}]\} \, ; \tag{31}$$

and for bubbles with $m = -1$, $b_{-1} > 0$

$$F = (1 + \bar{t}^2) \, (1 - \bar{t}^{1/2}) - (2 \, \bar{t}/3) \, (1 - \bar{t}^{3/2}) \, . \tag{32}$$

Here $\bar{t} = t / t_c$, t_c being given by equation (15) in equations (30 to 32) and $t_c = r_c^{-2} \, h / k_s$ in equation (29). Equations (29 to 31) are graphically represented in figure 4. As expected, all bubbles disappear within a finite time ($F = 0$ at $t = t_c$) if their growth rate is constant or proportional to r^{-1}. If their growth rate is zero or accelerated, they tend to persist. Then $N \to 0$ as $t \to \infty$ if $r = \text{const.}$ and $N \to \text{const.}$ ($F \to 1/2$) if $m = 2$ ($b_2 > 0$).

Bastick [19], Cable [20], van Erk et al. [7], and Mulfinger [1] reported that their data fit the exponential decrease in bubble count,

$$N = N_0 \exp(-K \, t) \, , \tag{33}$$

where N_0 and K are constants. According to this empirical relation, bubbles can be found in the melt at any time, however long. To fit this behavior with the power-law model, very small bubbles must be present initially and m must be larger than 1, so that the initially small bubbles can survive. Using equation (27), it is possible to find the initial bubble size distribution leading to an exponential decrease in the bubble count for any value of m compatible with the existence of bubbles in the liquid as $t \to \infty$. This can be easily done for the case of constant bubble size. Assuming that $r_{\min} = 0$ and using the fact that $N_r(r_h) = 0$ (i.e., all bubbles of $r \geq r_h$ have left the liquid), first and second differentiation of equation (27) with respect to time lead to

$$\dot{N} = \int_0^{r_h} \dot{N}_r \, dr \tag{34}$$

and

$$\ddot{N} = \int_{r_0}^{r_h} \ddot{N}_r \, dr + \dot{N}_r(r_h) \, r_h \, . \tag{35}$$

According to equations (19 and 23), $\dot{N}_r = - N_{r0} \, (k_s / h) \, r^2$ *and* $\ddot{N}_r = 0$. Recall that equation (18) expresses the time within which all bubbles of radius r initially situated in the depth $x \leq h$ leave the liquid. Rewritten as $r_h = (k_s / h)^{1/2} \, t^{-1/2}$ (that is, shifting the subscript h from t to r), it expresses the maximum radius of bubbles present in the liquid at time t. Now $\dot{r}_h = - (1/2) \, (k_s / h)^{1/2} \, t^{-3/2}$, or

$\dot{r}_h = -(1/2)\,(k_s / h)\,r^3$. The subscript h was dropped from r in the last expression, in which $\dot{r}_h$ is the time rate of change of the radius of the largest bubbles within the liquid (this radius changes as the largest bubbles are continually disappearing) and r is the time-independent bubble radius (that will become the maximum radius as soon as all larger bubbles leave the liquid). Hence, equation (35) becomes

$$\ddot{N} = (1/2)\,N_{r0}\,(k_s / h)^2\,r^5. \tag{36}$$

Differentiating equation (33) twice with respect to time, using equation (18) to eliminate t (while disregarding the subscript h), and joining the result with equation (36), one obtains for the initial bubble size distribution

$$N_{r0} = 2N_0 (K\,h/k_s)^{-2} r^{-5} \exp\,(-r^{-2}\,K\,h/k_s). \tag{37}$$

Since N_{r0} cannot depend on K, h, or k_s, it follows that $(K\,h\,/\,k_s)^{1/2} = \text{const}$. If one defines $r_1 = (K\,h\,/\,k_s)^{1/2}$, equation (37) can be rewritten as

$$N_{r0} = 2\,N_0\,r_1^4\,r^{-5} \exp\,(-\,r_1^2\,/\,r^2)\,. \tag{38}$$

Using the Stokes formula, the decrease in bubble count constant is

$$K = k_1\,r_{1g}^2\,g\,/\,v\,h\,. \tag{39}$$

By equations (19, 23, and 37), the bubble size distribution at time t is

$$N_r = 2\,N_0\,[1 - (k_s / h)\,r^2\,t]\,r_1^4\,r^{-5} \exp\,(-\,r_1^2\,/\,r^2). \tag{40}$$

This function is graphically represented in figure 5. It has a maximum at

$$r_m = \sqrt{3}\,r_1\,[1+\hat{t}^{-1}-(1+\hat{t}^{-2}-(2/5)\,\hat{t}^{-1}+\hat{t}^{-2})^{1/2}]^{1/2}, \tag{41}$$

where $\hat{t} = (2\,k_s\,/\,5\,h)\,r_1^2\,t$. This example shows that an exponential decrease in the total bubble count is possible for constant size bubbles if their initial size distribution has a special form given by equation (40).

It can be expected that if the bubble size changes with time, another unique initial bubble size distribution can be found that would lead to an exponential decrease in bubble count. Such a unique initial distribution is unlikely to be satisfied in any real batch melting situation. A question arises as to whether a bubble growth or shrinkage rate function can be found that would result in the exponential decrease for an arbitrary initial distribution. An attempt is made with an example of exponential shrinkage, that is, $m = 1$ and $b_1 < 0$. Using equations (9, 19 and 20),

$$N_r = N_{r0}\,\{1-(k_s\,r_0^2/2\,h\,B_1)\,[1-\exp\,(-2\,B_1\,t)]\}, \tag{42}$$

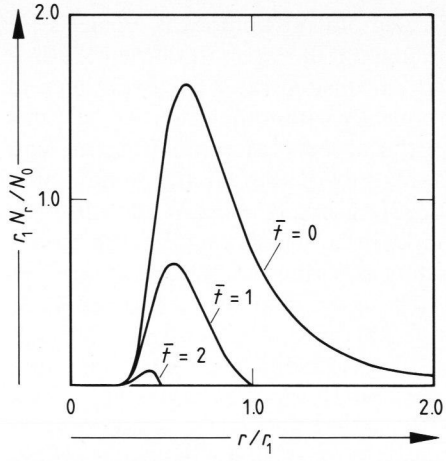

Figure 5. Bubble size distribution for constant bubble size and exponential decrease of bubble number.

where $B_1 = -b_1$. This equation becomes identical with equation (33) if $r_0 = (2\,B_1\,h\,/\,k_s)^{1/2}$, and so all bubbles must be of the same size. Thus, as in the previous example, the initial distribution cannot be arbitrary. Even though a single example does not constitute a mathematical proof, it seems unlikely that a function that would lead to the exponential decrease for an arbitrary initial distribution exists.

3. Discussion

The kinetics of bubble removal is determined by the initial bubble size distribution, N_{r0}, and the size history of individual bubbles during their passage through the melt. These constitutive characteristics can be deduced using bubble removal data and an appropriate model. This is analogous to viscosity calculation from viscometric data and the Navier-Stokes equation. Published reports on bubble removal provide the following information: the total bubble count as a function of time, $N(t)$ [1 and 19]; the time change of the bubble size distribution, $N_r(t)$ [20]; and the maximum bubble size, $r_h(t)$ [7]. The main findings of the most detailed experimental data can be summarized as follows:

a) bubbles can be found in the melt even after a long experimental time,

b) the maximum bubble size does not approach zero as time progresses, and

c) the minimum bubble size does not increase with time.

These features can be reproduced by the power-law model if $b_m > 0$ and $1 \le m < 3$. This agrees with van Erk et al. [7] who found that $m = 7/4$ provided the best fit of the power-law model to their data. Suprisingly, the conclusion that $b_m > 0$ and $1 \le m < 3$ rules out the possibility that bubbles shrink, have a constant size, grow at a constant rate, or, as theoretical analysis suggests [21], grow with the rate proportional to r^{-1}.

One of the ruled-out possibilities is Němec's [5] fundamental finding that during most of their lifetime bubbles grow with a constant rate. The experimental value of b_0 lies typically within the range $2 \cdot 10^{-8}$ m/s (slow growth in the absence of refining agent) and $2 \cdot 10^{-6}$ m/s (rapid growth due to the action of a refining agent) [22]. Using $h = 0.1$ m, $\eta = 10$ Pa s, and $\varrho = 2.5 \cdot 10^3$ kg/m^3 and assuming that the Stokes formula adequately describes bubble rise, one obtains $k_s = (2/9)\, \varrho\, g / \eta = 545$ m^{-1} s^{-1}. By equations (15 and 16), $r_c = 220$ μm and $t_c = r_c / b_0 = 183$ min in the case of slow growth, and $r_c = 1$ mm and $t_c = 8.6$ min in the case of rapid growth. All bubbles must leave the liquid by the time t_c at which their radius approaches r_c (t_c and r_c are indicated by the dotted lines in figure 2b). This prediction clearly disagrees with the bubble removal trials in which bubbles were found after times much longer than t_c, and their radii were considerably smaller than r_c.

If the value of m lies in the range between 1 and 3, the power-law model allows the bubbles to exist in the size range $0 < r \leq r_c$ as $t \rightarrow \infty$ (figures 2d and 3c). In reality, very small bubbles cannot grow because of the capillary forces. The real initial minimum bubble size can be stimated as $r_{0\min} = 2\,\sigma / \Delta p$, where σ is the surface tension and Δp the oversaturation pressure of the gas in the liquid. Bubbles with radius smaller than $r_{0\min}$ will dissolve. Using $\sigma = 0.3$ N/m and $\Delta p = 10^5$ Pa, $r_{0\min} = 6$ μm is obtained. Since much higher oversaturation pressures are possible, $r_{0\min} = 6$ μm is a conservative estimate. To estimate the rate coefficient b_m, let $m = 2$ and $r_c = 300$ μm. Equation (16) yields $b_2 = r_c\, k_s / h = 1.6$ m^{-1} s^{-1}, with the same values for h and k_s as in the previous example. By equation (8), the minimum bubble size is 6.5 μm after 2 h and 7.3 μm after 5 h. The maximum bubble size is 420 μm after 1 h, and 330 μm after 5 h. By equations (11 and 13), the total refining time is $t_t = h(r_{0\min}\ r_h\, k_s)^{-1} = 28$ h, where the radius of the last bubbles leaving the melt is, by equations (13 and 16), $r_h = r_{0\min} + r_c = 306$ μm. Refining experiments usually take 1 to 2 and rarely exceed 5 h. Within this time interval, the predicted bubble size range matches the experimental observation satisfactorily.

Accordingly, if no bubbles are generated at $t > 0$, the long residence time of some bubbles in the liquid is attributed by the power-law model to slow initial growth of small bubbles. These bubbles begin to grow quickly at the end of their lifetime, so they attain a relatively large size before they reach the top surface. However, a paradox arises in that the growth exponent $m \in (1,3)$ agrees neither with direct observation of bubble behavior nor with theoretical reasoning, which is based on the well-understood mechanism of growth or dissolution of a single bubble. Before suggesting what may be a possible cause of this paradox, some more details of bubble removal behavior will be discussed.

Cable [20] and van Erk et al. [7] found that any size fraction of bubbles decreased exponentially, that is,

$$N_r = N_{r0} \exp(-K_r t)\,, \tag{43}$$

where K_r is a function of r. This equation provokes three comments. First, it implies that the total bubble count, $N = {}_0\!\int^r N_{r0} \exp(-K_r t)\, \mathrm{d}r$, cannot decrease exponentially with time unless $K_r = K = $ const.; that is, K is independent of r, which is contrary to observation. A non-exponential decrease in the total bubble count is, therefore, more likely to occur and has been observed, for example by Cable [20]. Second, equation (43) is not compatible with Cable's suggestion that small bubbles dissolve and large bubbles grow [6]. This would imply the existence of medium-sized bubbles that neither grow nor shrink and their number would, by equation (23), decrease linearly with time. Third, by equations (19 and 20), relation (43) implies that

$$r = (h\, K_r / k_s)^{1/2} \exp(-K_r t / 2)\,. \tag{44}$$

Comparison of this equation with equation (9) reveals that $m = 1$, $K_r = r_0^2\, k_s / h$, and $b_1 = -r_0^2\, k_s / 2\, h$; that is, bubbles exponentially shrink with the rate coefficient related to the liquid depth, which can only be fortuitous. Furthermore, if $K_r = K = $ const., there is only one initial bubble radius possible. Hence, equation (43) is too restrictive to be generally valid.

Summarizing, three problems with bubble removal interpretation have been revealed. First, the exponential decrease in the total bubble count requires a special initial bubble size distribution which is unlikely to exist in reality (given by equation (38) for $r = $ const.). Second, discrepancies exist in connection with equation (43). Third, the decrease in bubble count found in laboratory crucible melts, which admits only accelerated growth rate of bubbles, is not compatible with the constant growth rate of individual bubbles observed by Němec [5]. It is possible that the first and second discrepancies result from extension of approximation functions, such as the exponential function, beyond the experimental range of data. However, the third discrepancy is of a more fundamental nature. A logical way this paradox can be resolved is by modifying some of the assumptions on which the model rests. The assumption most likely to be inadequate is that of no bubble formation in crucible melts after the batch-free time. Suppose that new bubbles are nucleated on container walls or within the melt and these new bubbles grow linearly with time. Their $r(t)$ functions can be represented as straight lines crossing the time axis at $t > 0$. The power-law model will see these straight lines as parabolas represented by equation (9), to which the corresponding straight lines are tangents.

This means that formation of a bubble at $t > 0$ is interpreted as a delayed growth of a small bubble present from the beginning of the refining process.

These two interpretations have serious consequences regarding the application of the data obtained from refining experiments conducted in laboratory crucibles to the refining process in glassmelting furnaces. In a furnace, no significant generation of bubbles is possible after all solid batch particles are dissolved and, therefore, the real refining times will be considerably shorter than those predicted from crucible experiments if bubbles indeed grow linearly in isothermal melts. To clarify this problem, experimental study is needed that would examine nucleation of bubbles on container walls. This would make it possible to separate removal of crucible-generated bubbles from those nucleated on batch particles prior to their dissolution, and thus obtain a better insight into the complex problem of bubble removal from molten glasses.

4. References

[1] Mulfinger, H. O.: Gase (Blasen) in der Glasschmelze. In: Jebsen-Marwedel, H.; Brückner, R. (eds.): Glastechnische Fabrikationsfehler. Berlin, Heidelberg, New York: Springer 1980. p. 193–268.

[2] Busby, T. S.: Gas bubbles from refractories. Glass Technol. **20** (1979) no. 3, p. 91–95.

[3] Němec, L.; Žlutický, J.: Photographic investigation of some processes occuring in glass melts. (Orig. Czech.) Sklář Keram. **29** (1979) no. 12, p. 353–358.

[4] Cable, M.; Clarke, A. R.; Haroon, M. A.: The influence of size of melt on the refining of a glass. Glass Technol. **9** (1968) no. 4, p. 101–104.

[5] Němec, L.: The refining of glass melts. Glass Technol. **15** (1974) no. 6, p. 153–156.

[6] Cable, M.: A study of refining. Pt. 2//Mechanisms of refining. Glass Technol. **2** (1961) no. 2, p. 60–70.

[7] Erk, K. van; Papanikolau, E.; Pelt, W. van: The effect of fluorides on antimony refining. In: XIth International Congress on Glass, Prague 1977. Proc. Vol. 4. Prague: Dum tech. 1977. p. 137–146.

[8] Němec, L.: Refining of glass melts. (Orig. Czech.) Silikaty **24** (1980) no. 4, p. 369–383.

[9] Weinberg, M. C.; Onorato, P. I. K.; Uhlmann, D. R.: Behavior of bubbles in glassmelts: I. Dissolution of a stationary bubble containing a single gas. J. Am. Ceram. Soc. **63** (1980) no. 3–4, p. 175–180.

[10] Weinberg, M. C.; Onorato, P. I. K.; Uhlmann, D. R.: Behavior of bubbles in glassmelts: II. Dissolution of a stationary bubble containing a diffusing and a nondiffusing gas. J. Am. Ceram. Soc. **63** (1980) no. 7–8, p. 435–438.

[11] Onorato, P. I. K.; Weinberg, M. C.; Uhlmann, D. R.: Behavior of bubbles in glassmelts: III. Dissolution and growth of a rising bubble containing a single gas. J. Am. Ceram. Soc. **64** (1981) no. 11, p. 676–682.

[12] Weinberg, M. C.; Subramanian, R. S.: Dissolution of multicomponent bubbles. J. Am. Ceram. Soc. **63** (1980) no. 9–10, p. 527–531.

[13] Cable, M.; Frade, J. R.: Theoretical analysis of the dissolution of multi-component gas bubbles. Glastech. Ber. **60** (1987) no. 11, p. 355–362.

[14] Cable, M.; Frade, J. R.: The diffusion-controlled dissolution of spheres. J. Mater. Sci. **22** (1987) no. 5, p. 1894–1900.

[15] Beerkens, R. G. C.: Behavior of single gas bubbles during refining of glass melt//Model studies for different oxidation states. (In prep.)

[16] Němec, L.; Mühlbauer, M.: Verhalten von Gasblasen in der Glasschmelze bei konstanter Temperatur. Glastech. Ber. **54** (1981) no. 4, p. 99–108.

[17] Mühlbauer, M.; Němec, L.: Einfluß der Gase einer Glasschmelze auf das Verhalten der Gasblasen unter isothermen Bedingungen. Glastech. Ber. **54** (1981) no. 12, p. 389–399.

[18] Němec, L.: Refining in the glassmelting process. J. Am. Ceram. Soc. **60** (1977) no. 9–10, p. 436–440.

[19] Bastick, R. E.: Laboratory experiments on the refining of glass. In: Symposium sur l'Affinage du Verre. Paris 1955. Charleroi: Union Scientifique Continentale du Verre 1956. p. 127–138.

[20] Cable, M.: A study of refining. Pt. 1//Measurement of the refining of a soda-lime-silica glass with and without refining agents. Glass Technol. **1** (1960) no. 4, p. 144–154.

[21] Scriven, L. E.: Dynamics of phase growth. Chem. Eng. Sci. **10** (1959) no. 1, p. 1–13.

[22] Němec, L.: Study of glass refining. Pt. 2//Contribution of the diffusion processes to the refining of glasses. (Orig. Czech.) Sklář Keram. **23** (1973) no. 9, p. 232–237. 89R0586